THE JOURNAL OF PHYSICAL CHEMISTRY B

AMOLF

B: Liquids, Chemical and Dynamical Processes in Solution, Spectroscopy in Solution

Vibrational Relaxation Dynamics of the Core and Outer Part of Proton-Hydration Clusters

Oleksandr Oleksandrovich Sofronov, and Huib J. Bakker

J. Phys. Chem. B, **Just Accepted Manuscript** • DOI: 10.1021/acs.jpcb.9b02067 • Publication Date (Web): 02 Jul 2019

Vibrational Relaxation Dynamics of the Core and Outer Part of Proton-Hydration Clusters

Oleksandr O. Sofronov* and Huib J. Bakker

AMOLF, Science Park 104, 1098 XG Amsterdam, The Netherlands

e-mail: sofronov@amolf.nl

ABSTRACT

We study the ultrafast relaxation dynamics of hydrated proton clusters in acetonitrile using femtosecond mid-infrared pump-probe spectroscopy. We observe a strong dependence of transient absorption dynamics on the frequency of excitation. When we excite the OH vibrations with frequencies $\leq$3100 cm^{-1} we observe an ultrafast energy relaxation that leads to heating of the local environment of proton. This response is assigned to the OH vibrations of the water molecules in the core of the hydrated proton cluster. When we excite with frequencies $\geq$3200 cm^{-1} we observe a relatively slow vibrational relaxation with a T_1 time constant ranging from 0.22±0.04 ps at ν_{ex}=3200 cm^{-1} to 0.37±0.02 ps at ν_{ex}=3520 cm^{-1}. We assign this response to water molecules in the outer part of the hydrated proton cluster.

INTRODUCTION

The proton (H^+) plays a key role in various chemical processes in aqueous media.[1–4] For the proton in liquid water different solvation structures have been proposed, including the $H_3O^+(H_2O)_3$ Eigen cation, the $H_5O_2^+$ Zundel cation and the so-called asymmetric Zundel as an intermediate geometry of the first two. These structures are based on cryogenic photodissociation vibrational spectroscopy experiments of small protonated water clusters,[5,6] and molecular dynamics simulations.[7–9] In the cluster experiments Eigen and Zundel cation structures have been identified from the central frequencies of the OH-stretch vibrations. However, quantitative infrared spectroscopy[10,11] and photodissociation spectroscopy of large protonated water clusters[5,12,13] as well as molecular dynamics simulations[9,14–16] show that the water molecules in the second solvation shell of the proton also possess different properties from the molecules in bulk water, which implies that the Eigen and Zundel cations only represent the central cores of the proton-hydration structures in liquid water.

Infrared spectroscopy is a powerful technique for studying strongly hydrogen-bonded systems like the hydrated proton, since the vibrational frequency of the stretch vibration of the hydrogen-bond donating group strongly depends on the strength of the donated hydrogen bond.[4,17] A complication is that strong hydrogen bonding leads to extremely broad absorption bands for the OH-stretch vibration. As a result, the hydrated proton in liquid water shows a nearly continuous absorption spanning from 1000 cm^{-1} to 3600 cm^{-1}.[18–20] Recent *ab initio* molecular dynamics simulations show that the large width of the absorption band largely results from the heterogeneity of the hydrogen bonds, in particular the difference in hydrogen-bond strength between the water molecules in the first and the second hydration shells.[21]

Femtosecond infrared (fs-IR) spectroscopy provides information on the relaxation dynamics and can thereby help in the assignment of the different regions of the absorption spectrum of the OH-stretch vibrations of the hydrated proton. Femtosecond IR spectroscopy have recently been used to study the properties of hydrated proton clusters in acetonitrile.[22–24] Acetonitrile as a weakly polar solvent is a very suitable matrix for hydrated proton clusters.

In Ref. 23 it was proposed that in a system of acid water in acetonitrile with a ratio $[H^+]:[H_2O]=1:3$, the proton is mainly found in between two water molecules (not necessarily in a symmetric configuration), forming a Zundel $H_5O_2^+$ structure. This finding agrees with the results of earlier linear infrared[25] and ^1H NMR[26] studies and a fs-IR study of the proton transfer mode.[24] Using excitation pulses centered at 2700 cm^{-1} it was concluded that the excited central OH-stretch vibration of the Zundel-like structure relaxes ultrafast with a time constant $T_1<65$ fs.[23] The relaxation following excitation at 3400 cm^{-1} was also observed to be ultrafast with an upper limit for T_1 of 50 fs. This relaxation behavior was assigned to the OH vibrations of the two H_2O molecules flanking the Zundel proton. It was also shown in this study that the fluctuations of the electrical interactions between the hydrated proton and the surrounding acetonitrile molecules strongly modulate the hydration structure geometry and the vibrational potential of the Zundel proton on an ultrafast scale.[23,24]

Ottosson et al.[22] investigated the picosecond dynamics of hydrated protons in acetonitrile. In this study it was found that the relaxation of the excited proton partly results in the ultrafast creation (<100 fs) of a locally hot proton hydration cluster, and partly in the vibrational predissociation of a hydrogen bond of the cluster and the release of a water molecule. The reassociation of this bond was observed to occur with a time constant of ~6 ps.

Here we present a comparative femtosecond mid-infrared pump-probe spectroscopic study of the vibrational dynamics of the core and outer parts of hydrated proton clusters in acetonitrile. An important difference between the present study and earlier work is that we resolve the frequency-dependent vibrational relaxation time constants of the OH-stretch vibrations of the outer part of the hydration structure. In the work by by Dahms et al.[23] this relaxation was believed to be ultrafast (< 50 fs). We find that for excitation frequencies >3100 cm^{-1} the relaxation is much slower (220-370 fs) and strongly depends on frequency, which implies that the OH-stretch vibrational spectrum of the outer part of the proton hydration structure is strongly inhomogeneously broadened.

EXPERIMENT

We measured transient absorption spectra using independently tunable femtosecond mid-infrared pump and probe pulses.[27] The pump and probe pulses are generated using optical parametric amplifiers (OPAs) that are pumped with the 800 nm 35 fs pulses produced by a regenerative Ti:sapphire amplifier (Coherent) with 3.5 mJ energy per pulse. To generate the probe pulses we pump a homebuilt OPA based on a β-barium borate (BBO) crystal with 1 mJ of the 800 nm pulse energy. The OPA process is seeded with white light. After two amplification stages the OPA delivers signal and idler pulses with a total energy of 220 μJ. The signal and idler pulses are mixed in a silver gallium disulfide (AGS) crystal to produce mid-infrared pulses at their difference frequency. The resulting pulses are transmitted through a germanium filter to remove residual signal and idler light, and through calcium fluoride windows to compensate the group velocity dispersion introduced by germanium. The resulting pulses have a central frequency that is tunable in the range 2700-3500 cm^{-1}, a spectral full width at half maximum of 300 cm^{-1}, and a pulse

duration of 60 fs. The pulses are split into probe and reference pulses using wedged zinc selenide windows. The probe beam was sent through a delay stage to introduce a variable time delay with respect to the pump pulse.

The pump pulses are produced by another OPA based on a β-barium borate (BBO) crystal that is pumped with a fraction of 1.3 mJ of the 800 nm beam. The resulting idler beam is frequency doubled using another BBO-crystal. Subsequently, the second harmonic of the idler is used as a seed in a second OPA process in a potassium titanyl phosphate (KTP) crystal that is pumped with a fresh fraction of 1 mJ of the 800 nm pulse. This OPA process leads to amplification of the doubled idler and the production of pulses at the difference frequency. The latter pulses (Figure 1A) are tunable in the range 2900-3500 cm^{-1} and have a spectral full width at half maximum of ~150 cm^{-1}, a pulse duration of ~120 fs and an energy of 15-20 μJ. The polarization of the pump beam is set at 45° with respect to the probe polarization using a half-wave plate. The pump pulses are focused into the sample in spatial overlap with the probe pulses.

After the sample, we select the polarization component of the probe and reference beams that is either parallel or perpendicular to the pump polarization with a polarization filter. Subsequently, the probe and the reference beams are dispersed by a spectrometer and detected by two lines of a 3x32 mercury-cadmium-telluride infrared detector array. To obtain transient absorption change spectra $\Delta\alpha_{\parallel}(\nu,t)$ and $\Delta\alpha_{\perp}(\nu,t)$, every second pump pulse was mechanically chopped. From the measured parallel and perpendicular components we construct the isotropic signal, which is independent of the transition dipole moment reorientation

$$\Delta\alpha_{iso}(\nu,t) = \frac{1}{3}\left(\Delta\alpha_{\parallel}(\nu,t) + 2\Delta\alpha_{\perp}(\nu,t)\right) \quad (1)$$

The samples are prepared by dissolving trifluoromethanesulfonic acid (TfOH, 99%, Sigma-Aldrich) in water and deuterated acetonitrile (CD_3CN, 99.8%, Sigma-Aldrich) at a ratio

TfOH:H_2O:CD_3CN=1:3:75. Previous IR pump-probe[22] and FTIR[23,25] studies showed that the nature of the counter-ion ($CF_3SO_3^-$, ClO_4^- or I^-) does not have a significant influence on the structure and dynamics of the hydrated proton in acetonitrile. The solution is put in between two 2 mm thick calcium fluoride windows separated by a 50 μm Teflon spacer. The nonresonant signal due to pump-probe cross-phase modulation in the calcium fluoride windows limits the experimental time resolution to ~0.2 ps. In some of the experiments we obtained a better time resolution by using 500 nm thick silicon nitride windows instead of calcium fluoride windows.

RESULTS AND DISCUSSION

Transient spectra and delay time traces

In Figure 1B we show transient absorption spectra following excitation with pulses centered at 3300 cm^{-1}. In Figure 1C,D we show isotropic transient absorption spectra obtained with different central excitation frequencies at two different delay times (0.24 ps and 20 ps). At an early delay time of 0.24 ps, the transient absorption spectrum strongly depends on the excitation frequency. Excitation with a high-frequency excitation pulse ($\nu_{ex} \geq 3300$ cm^{-1}) leads to a small positive absorption change at low frequencies. Excitation at frequencies ≤ 3200 cm^{-1} leads to a decreased absorption below 3500 cm^{-1} and an enhanced absorption at probe frequencies >3500 cm^{-1}. This spectral shape is similar to the transient absorption spectrum observed at long delay times (>10 ps) for all different excitation frequencies. This spectrum consists of a positive absorption change at frequencies >3600 cm^{-1} and a broad negative absorption change at lower frequencies.

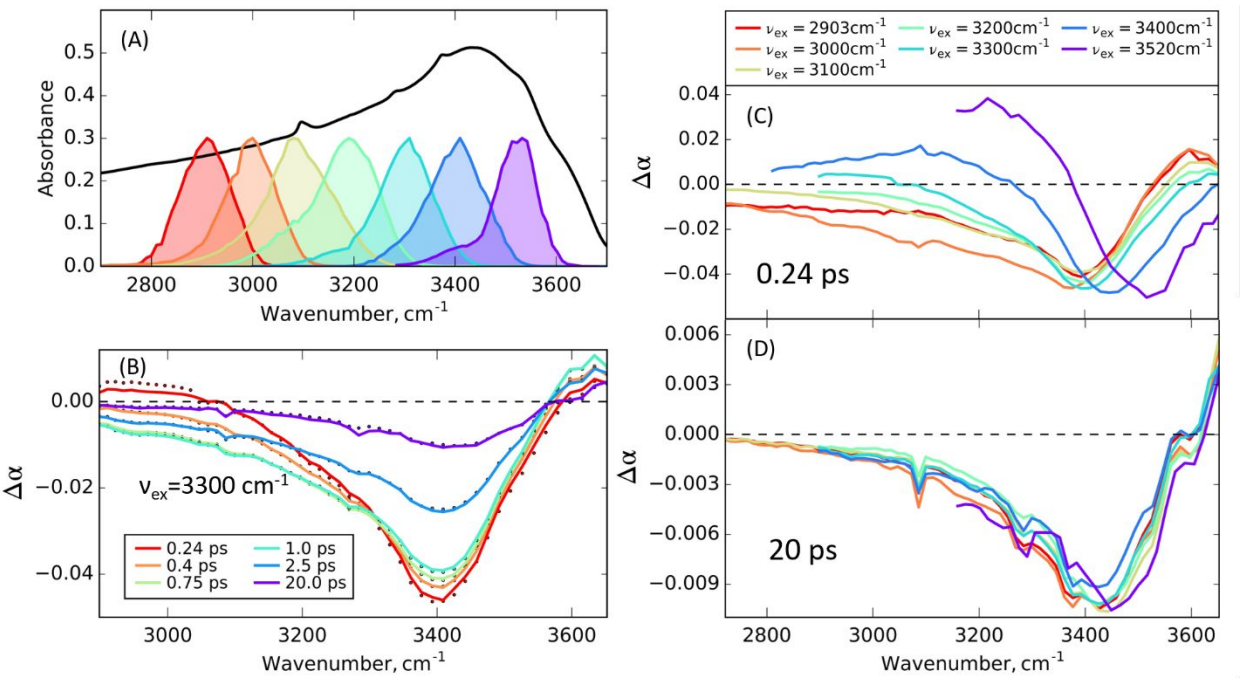

Figure 1. (A) Linear infrared absorption spectrum of the TfOH:H_2O=1:3 mixture in acetonitrile-d3 (black line, solvent background subtracted) and pump pulses used in the experiments (color lines). (B) Isotropic transient spectra of the hydrated proton in acetonitrile with ν_{ex}=3300 cm^{-1} (lines represent the result of the fit). (C,D) Isotropic pump-probe spectra at the delay times of 0.24 ps (C) and 20 ps (D) with excitation frequency varied.

Coherent coupling effects

In a previous study of hydrated protons in acetonitrile an intense increase of the induced absorption within the pump-probe cross-correlation time was observed.[23] This signal was assigned to Zundel cations excited at 3400 cm^{-1}. Since the observed signal was present only within the cross-correlation of the pump and probe pulses, the authors concluded that the excited state lifetime of these Zundel cations should be below 50 fs. The subsequent slower relaxation was assigned to energy redistribution within the Zundel cation.

In our studies we observed a similar fast signal component within the pump-probe cross-correlation time. However, we found the contribution of this signal component to be strongly dependent on the difference between the central frequency of the probe pulse and the frequency at which the transient absorption signal was detected. In Figure 2 we show the early delay time dynamics of the induced absorption signal at 3160 cm^{-1} measured with different probe pulses. After 0.2 ps the transient signal purely consists of the excited state absorption and heating signatures. These signals are independent of the central frequency of the probe pulse. However, in the time interval between -0.1 and 0.2 ps we find that the transient absorption signal becomes increasingly distorted when the detection frequency is shifted further away from the central frequency of the probe pulse. This behavior can be well explained from the additional signal contributions that arise from coherent coupling effects when the pump and probe pulses overlap in time. The origin and impact of these coherent effects are discussed in detail in the Supporting information.

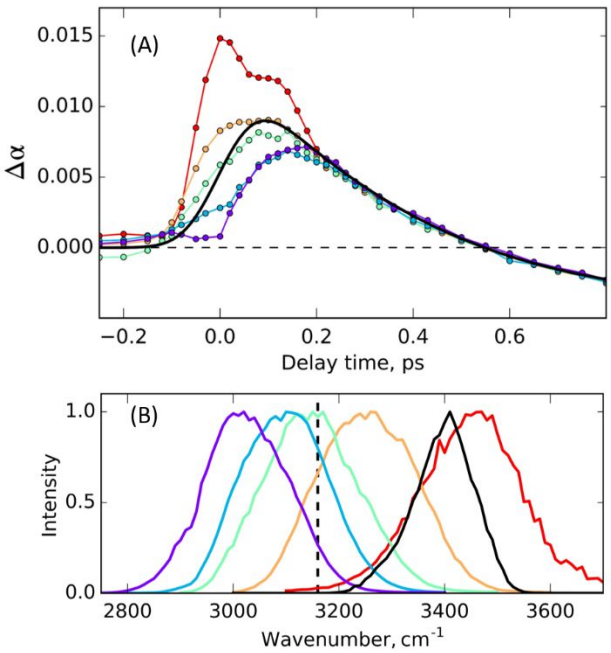

Figure 2. (A) The fast transient absorption dynamics at frequency 3160 cm^{-1} measured with various probe pulses; black line represents the fit. (B) Intensity spectra of the probe pulses used (color lines) and the pump pulse (black line).

When the spectrum of the probe pulse is centered at the frequency of maximum of the linear absorption, i.e. the frequency of the fundamental v=0→1 transition, a strong coherent coupling effect in the region of the excited state absorption (red curve in Figure 2A). This coherent-coupling signal has the form of an additional positive signal and can be easily mistaken for the contribution of an ultrafast decaying excited state. We find that this strong additional positive signal vanishes if the spectrum of the probe pulse is centered close to the frequency of interest (green curve in Figure 2A). Therefore, we conclude that excitation at 3400 cm^{-1} results only in the excitation of relatively slowly relaxing water OH-stretch vibrations. In view of the frequency of 3400 cm^{-1} these OH vibrations are likely not located in the core of the proton hydration cluster but in the outer part of this structure..

Vibrational relaxation dynamics following excitation ≤3100 cm^{-1}

When we excite the solution with excitation pulses centered at 2900, 3000 and 3100 cm^{-1}, we observe at early delay times a very broad negative signal (bleaching) extending to lower frequencies (Figure 3A). The signal has a zero crossing at 3500 cm^{-1} and a positive sign (induced absorption) at frequencies >3500 cm^{-1}. Following earlier work[22,23] we explain the signal at early delay times from a strong local heating effect that results from the ultrafast relaxation of the excited OH-stretch vibrations.

We model the transient spectra obtained with $\nu_{ex} \leq 3100$ cm^{-1} with the kinetic model that was used in a previous study of protonated water clusters in acetonitrile.[22] Within this model the excited vibrational state relaxes to an intermediate state with a relaxation time constant that is too short to be resolved. This intermediate state of the relaxation represents the effect on the absorption of the proton hydration complex of the local dissipation of energy to the water molecules that surround the proton. We will denote this state as the local hot state.

In Figure 3B we show the transient absorption spectra at early delay times following excitation at 2900, 3000 and 3100 cm^{-1}. The spectral signatures with ν_{ex}=2900 and 3000 cm^{-1} consist of a broad negative absorption change below 3400 cm^{-1} and a positive absorption change around 3500 cm^{-1}. These spectra are similar to the previously obtained spectra with ν_{ex}=2700 and 2800 cm^{-1}.[22,23] The negative part of the spectrum depends on the excitation frequency, which implies that the relaxed energy affects mostly the originally excited vibrations.

The local hot complex relaxes to a second intermediate state that represents the heating of the whole protonated water cluster. The time constant of this relaxation is 0.26±0.04 ps, meaning that the hot proton complex redistributes its energy over the complete protonated water cluster on a time scale of hundreds of femtoseconds. This time constant agrees with the previously reported time constant of 0.32 ps of the energy redistribution following 2800 cm^{-1} excitation.[22] In the hot water cluster the hydrogen bonds are weaker, which induces a decrease of the OH-stretch absorption cross-section and a blue shift of the vibrational frequency. On a longer time scale, the hot cluster dissipates its energy to the acetonitrile solvent, resulting in a significant decrease of the amplitude of the heating signal and the appearance of sharp acetonitrile peaks and OH-stretch absorption features that can be assigned to monomeric water molecules.

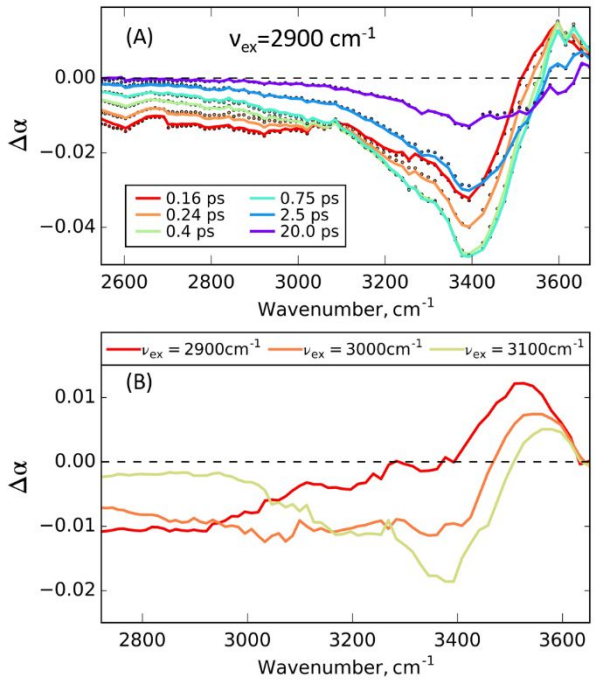

Figure 3. (A) Isotropic transient spectra of the hydrated proton in acetonitrile with ν_{ex}=2900 cm^{-1} (lines represent the result of the fit). (B) The transient spectral signatures of the local hot state after the low frequency excitation.

Vibrational relaxation dynamics following excitation at frequencies ≥3200 cm^{-1}

For excitation frequencies ν_{ex}>3300 cm^{-1} we observe a negative absorption change around 3400 cm^{-1} that we assign to the bleaching of the fundamental v=0→1 transition and stimulated v=1→0 emission of the excited OH-stretch vibrations. The positive absorption change below 3200 cm^{-1} is assigned to the corresponding v=1→2 excited state absorption.

The transient absorption spectrum also shows a fast growing spectral component corresponding to the transiently heated hydrated proton cluster. At 1 ps we observe a broad negative signal with a peak at ~3400 cm^{-1} and a small induced absorption around 3600 cm^{-1} (see

Figure 1B). This spectrum has a very similar shape as the spectrum that is observed after 1 ps for excitation frequencies $\nu_{ex} \leq 3100$ cm^{-1}, and that is observed at much later delay times, e.g. at 20 ps. Hence, we assign this spectrum to the response of the complete hot protonated water cluster.

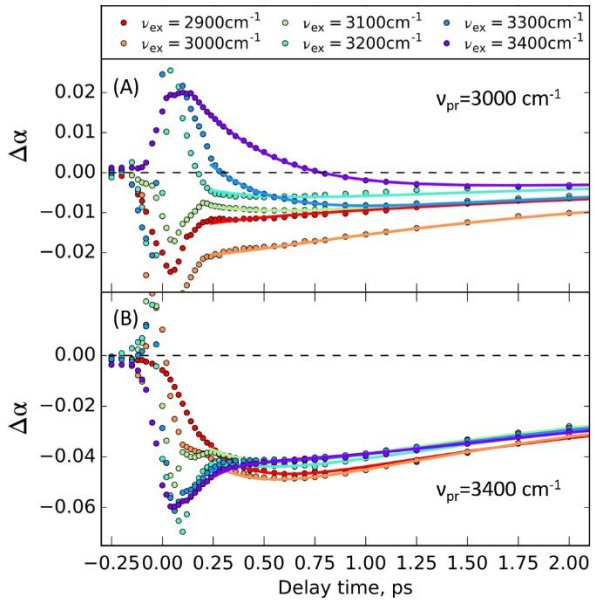

Figure 4. Isotropic pump-probe signal of the hydrated proton in acetonitrile at frequencies 3000 cm^{-1} (A) and 3400 cm^{-1} (B) as a function of delay time; excitation frequency varies from 2900 to 3400 cm^{-1}. Lines represent the result of the fit.

Because of its large transient spectral amplitude, the spectral response of the hot protonated water cluster becomes significant already at early delay times and dominates the initial positive absorption signal in the region of the v=1→2 excited state absorption. The transient signal at ν_{pr}=3000 cm^{-1} becomes negative at 0.7 ps for ν_{ex}=3400 cm^{-1}, and already at 0.3 ps for ν_{ex}=3300 cm^{-1} (Figure 4A). The transient absorption signal at ν_{pr}=3400 cm^{-1} (Figure 4B) shows a much slower decay because at this frequency, the initial signal has a negative sign as it is due to the v=0→1 bleaching and stimulated v=1→0 emission. At this detection frequency the vibrational

relaxation process replaces this initial negative signal by the negative absorption change associated with the hot cluster.

We fit the experimental data obtained with excitation frequencies ≥3300 cm^{-1} with a kinetic model that contains four states. The first state is the v=1 state of the OH-stretch vibration that is excited by the excitation pulse. The relaxation of this state results in heating of the protonated water cluster. We observe that the rise of this heating is somewhat delayed with respect to the relaxation of the excited v=1 state. It has been observed before in studies of the vibrational relaxation of bulk water that the heating signal grows somewhat slower than the excited vibration relaxes.[28,29] This delay is not observed when we excite low-frequency OH-stretch vibrations with $\nu_{ex} \leq 3100$ cm^{-1} (the local hot state is observed immediately), which indicates that the low- and high-frequency OH vibration have different relaxation mechanisms. The relaxation of the high-frequency OH vibration likely proceeds through an intermediate state with an associated response that is quite different from a local heating effect. To account for the delay of the heating effect following the relaxation of the high-frequency OH-stretch vibrations, we include in the model an intermediate state in between the excited v=1 state and the hot water cluster state. We did not include the relatively small and long living spectral component of the vibrational predissociation that has been observed before[22]. The hot cluster exchanges heat energy with its surrounding to reach the fourth state in the model which represents the eventual globally heated state of the system.

The relaxation dynamics of the OH-stretch excited state can be well estimated from the low frequency region, where v=1→2 excited state absorption is the dominant spectral component. Comparing the transient absorption dynamics in this frequency region (Figure 4A), we observe a strong difference between the results of excitation at 3400 cm^{-1} and at 3300 cm^{-1}. The initial signal

value at ν_{pr}=3000 cm^{-1} is much smaller when the oscillators are excited at lower frequency. This observation cannot be explained from a much faster relaxation of OH-stretch excited state, since the dynamics are similar to what is observed in the case of excitation at 3400 cm^{-1}. The observation of a small induced absorption signal at early delay times indicates that the hot cluster state is in part directly populated, i.e. in a separate relaxation channel that is faster than our time resolution. We thus conclude that the excitation pulse centered at 3300 cm^{-1} excites two types of OH oscillators. We find a good description of the transient spectra observed for ν_{ex}=3300 cm^{-1} when 40±10% of the excited OH vibrations relax very rapidly (T_1<50 fs) and directly populate the hot cluster state, and 60±10% relaxes more slowly with a time constant of 270±30 fs. For ν_{ex}=3200 cm^{-1} we find that 70±10% relaxes directly to the hot cluster state and 30±10% relaxes with a time constant of 220±40 fs.

In figure 5A we show the spectral signatures of the excited v=1 state extracted from the fit. The spectrum of the excited state shows a significant dependence on the excitation frequency: the position of the ground state bleach shifts from 3500 to 3380 cm^{-1}, and the excited state lifetime T_1 decreases from 370±20 fs at ν_{ex}=3520 cm^{-1} to 220±40 fs at ν_{ex}=3200 cm^{-1} (Figure 5B).

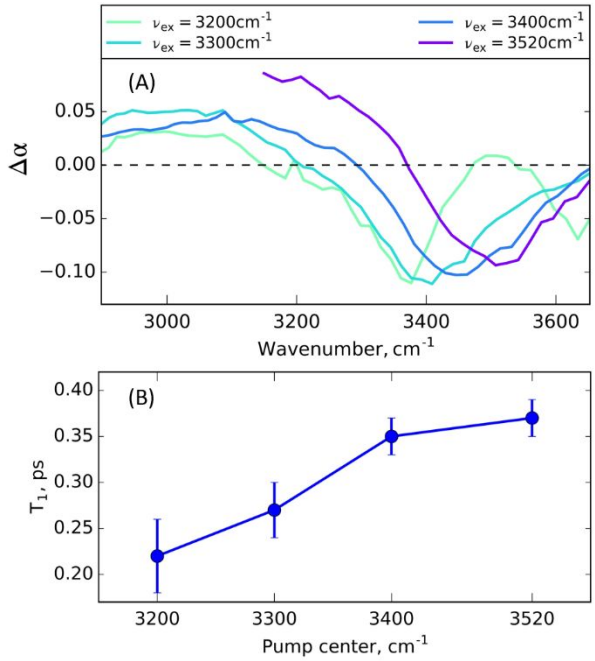

Figure 5. (A) Transient spectra associated with the excitation of the v=1 state of the OH-stretch vibration for four different excitation frequencies. (B) Time constant T_1 of the relaxation of the v=1 state as a function of the central excitation frequency.

The observed frequency dependence of the relaxation time constant indicates that the spectrum of the OH-stretch vibrations is inhomogeneously broadened. The variation of the excited state lifetime T_1 correlates well with the variation in local hydrogen-bond strength: OH-groups engaged in stronger hydrogen bonds have lower absorption frequencies and show faster relaxation. Interestingly, the dependence of the vibrational lifetime on the excitation frequency is very similar to that observed for bulk liquid water,[30] for which T_1 was found to decrease from 0.4 ps for ν_{ex}=3500 cm^{-1} to 0.25 ps for ν_{ex}=3200 cm^{-1}.

Discussion

We observe strongly different early delay time transient spectra when we shift the excitation frequency from 2900 cm^{-1} to 3520 cm^{-1}. This finding shows that the OH-stretch vibrational spectrum represents OH-groups of highly different character. At frequencies ≤3100 cm^{-1} we excite OH vibrations located in the core of the proton hydration cluster. For the (distorted) Zundel structure this core is formed by the OH-stretch vibration involving the central H atom in the $H_5O_2^+$ structure, for the Eigen structure the core is formed by the OH vibrations involving the three H atoms of the central H_3O^+ of the $H_9O_4^+$ structure. The main property of these OH vibrations that the H atom carries a significant part of the positive charge, and as a result donates a strong hydrogen bond. As a result, the frequency of these OH vibrations is <3200 cm^{-1} and the vibrational relaxation is ultrafast (<50 fs).

For excitation frequencies >3200 cm^{-1} the observed transient spectra resemble that of the OH-stretch vibration in neat water and hydrogen-bonded water in other media. The vibrational relaxation of this excited state is about 30 times faster than that of isolated water molecules in acetonitrile (T_1=8 ps)[31,32], and has a quite similar relaxation rate as the OH-stretch vibrations in bulk water.[30] From this we conclude that the observed high frequency OH-stretch vibrations belong to water molecules that belong to a cluster that contains at least one proton, but that are not in the center of the proton hydration structure, i.e. the H atoms involved in these OH vibrations do not carry a significant of the positive proton charge. At a concentration ratio of $[H^+]$:$[H_2O]$=1:3 the hydrated proton clusters in acetonitrile contain 2 to 6 water molecules.[26] The OH vibrations giving rise to this response can thus belong to the two H_2O molecules flanking the Zundel proton, or the OH vibrations of the three outer H_2O molecules of the Eigen $H_9O_4^+$ structure, or water molecules even further away from the core of the proton hydration structure. All these OH

vibrations have in common that the partial positive charge on the H atom is small and that they absorb at frequencies ≥3200 cm^{-1}.

Excitation at intermediate frequencies of 3100-3200 cm^{-1} yields spectral dynamics of intermediate character. We observe OH-stretch vibrations showing a fast but resolvable vibrational relaxation, and the direct creation of a local hot state. It thus follows that we observe quite distinct vibrational relaxation behavior of the core and the outer part of the proton hydration cluster, even in the spectral region where the spectra of the corresponding OH vibrations overlap.

Interestingly, the transient spectrum observed at long delay times and that we assign to the response of the entire hot water cluster, is the same irrespective of the original excitation frequency. This finding shows that all OH-stretch vibrations absorbing in the region from 3520 cm^{-1} to 2900 cm^{-1} belong to protonated water clusters that have similar absorption spectra and that are thus likely of similar composition.

Combining the results of all different excitation pulses we summarize the relaxation processes of the different OH-stretch vibrations in the protonated water cluster with the kinetic scheme shown in Figure 6. In this scheme, the v=1 state relaxes to a local hot state with a time constant T_1 that decreases with decreasing excitation frequency. The high frequency part (≥3200 cm^{-1}) of the spectrum corresponds to the OH-stretch vibrations of the water molecules in the outer part of the proton hydration cluster, which display the vibrational relaxation dynamics similar to that of bulk water. The lower frequency absorption of the protonated cluster is due to the vibrations of the core of the cluster, the excited state of which relaxes much faster. The absorption spectra of these two types of vibrations overlap in the frequency region of 3100-3300 cm^{-1}, and excitation pulses in this frequency region will thus excite both the core and the outer part of the proton hydration cluster. As a result, we observe mixed vibrational relaxation dynamics. For all OH

vibrations the relaxation results in a local hot state with a spectrum that depends on the excitation frequency. At lower frequencies this spectrum will primarily reflect the effect of local heat dissipation on the core of the proton hydration structure. At higher frequencies the spectrum of the local hot state is blueshifted and is very similar to that of the complete hot water cluster, i.e. the state that results after the heat has been equilibrated over the entire proton hydration cluster.

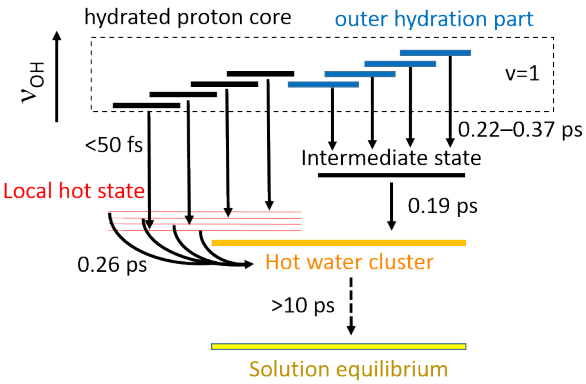

Figure 6. Kinetic scheme describing the spectral dynamics after excitation of the hydrated proton OH vibrations.

We note that the transient hot states observed in our experiments are very local in nature and differ from a true thermal state of the whole sample. As a result, these transient hot spectra differ from the linear thermal difference spectrum of the hydrated proton in acetonitrile. This latter spectrum shows a much broader negative absorption change than observed in the femtosecond experiments at delay time >10 ps.[22] An increase in the equilibrium temperature is observed to lead to a similar decrease of the cross-section for all OH-stretch vibrations (see Supporting Information). In contrast, the pump-probe spectrum at 1 ps shows predominant absorption changes in the frequency region of the outer part of the cluster even when the core of the cluster was initially excited. Apparently, the studied system does not reach complete thermal equilibrium within the

picosecond time frame of the pump-probe experiment. Similar observations were done for pump-probe experiments on the hydrated proton in DMSO[27] and in bulk water.[33,34] This discrepancy between the final thermal difference spectrum of the pump-probe experiment and the fully equilibrated response to heating of the sample can be explained from the fact that complete equilibration includes a change of the composition of the clusters. This change in composition involves diffusion and exchange of molecules between different clusters. These processes occur on much longer time scales than the picosecond times scale of the time-resolved experiments.

CONCLUSIONS

We studied the vibrational relaxation and energy dissipation of small protonated water clusters in acetonitrile using femtosecond mid-IR pump-probe spectroscopy. We find that the relaxation dynamics strongly depend on the excitation frequency. Excitation of the low frequency part of the OH-stretch band ($\leq$3100 cm^{-1}) is followed by ultrafast vibrational relaxation (T_1<50 fs), resulting in a local energy dissipation that affects mostly the originally excited vibrations. The transient spectrum of this local hot state shows a broad negative absorption change around the excitation frequency. After the fast vibrational relaxation of these OH groups the energy equilibrates over the complete protonated water cluster with a time constant of 0.26±0.04 ps.

Excitation of the high-frequency part of the OH-stretch band ($\leq$3200 cm^{-1}) is followed by vibrational relaxation of the OH-stretch vibration with a time constant ranging from T_1=0.22±0.04 ps for an excitation pulse centered at 3200 cm^{-1} to T_1=0.37±0.02 ps for an excitation pulse centered at 3520 cm^{-1}. We found that the signal previously assigned to the relaxation of the Zundel cation excited at 3400 cm^{-1} strongly depends on the probe pulse and originates from the coherent coupling of pump and probe pulses. The vibrational relaxation results in a somewhat delayed heating of the

complete protonated water cluster, which indicates that the high-frequency OH-stretch vibrations have a different relaxation mechanism, i.e. proceed through a different intermediate state in comparison with the low-frequency OH-stretch vibrations.

The spectrum of the hot protonated water cluster that results after relaxation of the high-frequency OH vibrations is the same as is observed after excitation of the low-frequency OH-stretch vibrations. This result shows that the high- and low-frequency OH vibrations belong to the same type of protonated water clusters. We thus assign the low-frequency part of the OH spectrum to the core of the proton hydration cluster and the high-frequency part of this spectrum to the outer part of this cluster. At intermediate excitation frequencies between 3100 cm^{-1} and 3300 cm^{-1} we do not observe average or intermediate behavior but two distinct relaxation components. Part of the OH vibrations show the ultrafast relaxation behavior of the core while the other part shows the relatively slower relaxation dynamics of the outer part. This latter fraction increases with increasing excitation frequency. We conclude that the core shows quite distinct vibrational relaxation behavior from the outer part, even in the spectral region where the spectra of the corresponding OH vibrations overlap.

SUPPORTING INFORMATION

Discussion of the impact of the coherent effects on the measured pump-probe signal; comparison of the linear thermal difference spectrum and the pump-probe spectra at different delay times.

ACKNOWLEDGMENTS

This work is part of the research program of the Netherlands Organization for Scientific Research (NWO) and was performed at the research institute AMOLF. This project has received funding from the European Research Council (ERC) under the European Union's Horizon 2020 research and innovation program (grant agreement No 694386). The authors thank Dr. Jan Versluis and Hinco Shoenmaker for the experimental support.

REFERENCES

(1) Kreuer, K. D. Proton Conductivity: Materials and Applications. *Chem. Mater.* **1996**, *8*, 610–641.

(2) Garczarek, F.; Gerwert, K. Functional Waters in Intraprotein Proton Transfer Monitored by FTIR Difference Spectroscopy. *Nature* **2006**, *439*, 109–112.

(3) Voth, G. A. Computer Simulation of Proton Solvation and Transport in Aqueous and Biomolecular Systems. *Acc. Chem. Res.* **2006**, *39*, 143–150.

(4) Agmon, N.; Bakker, H. J.; Campen, R. K.; Henchman, R. H.; Pohl, P.; Roke, S.; Thämer, M.; Hassanali, A. Protons and Hydroxide Ions in Aqueous Systems. *Chem. Rev.* **2016**, *116*, 7642–7672.

(5) Headrick, J. M.; Diken, E. G.; Walters, R. S.; Hammer, N. I.; Christie, R. A.; Cui, J.; Myshakin, E. M.; Duncan, M. A.; Johnson, M. A.; Jordan, K. D. Chemistry: Spectral Signatures of Hydrated Proton Vibrations in Water Clusters. *Science* **2005**, *308*, 1765–1769.

(6) Wolke, C. T.; Fournier, J. A.; Dzugan, L. C.; Fagiani, M. R.; Odbadrakh, T. T.; Knorke, H.; Jordan, K. D.; McCoy, A. B.; Asmis, K. R.; Johnson, M. A. Spectroscopic Snapshots of the Proton-Transfer Mechanism in Water. *Science* **2016**, *354*, 1131–1135.

(7) Marx, D.; Tuckerman, M. E.; Hutter, J.; Parrinello, M. The Nature of the Hydrated Excess Proton in Water. *Nature* **1999**, *397*, 601–604.

(8) Kulig, W.; Agmon, N. A "clusters-in-Liquid" Method for Calculating Infrared Spectra Identifies the Proton-Transfer Mode in Acidic Aqueous Solutions. *Nat. Chem.* **2013**, *5*, 29–35.

(9) Markovitch, O.; Chen, H.; Izvekov, S.; Paesani, F.; Voth, G. A.; Agmon, N. Special Pair Dance and Partner Selection: Elementary Steps in Proton Transport in Liquid Water. *J. Phys. Chem. B* **2008**, *112*, 9456–9466.

(10) Śmiechowski, M.; Stangret, J. Proton Hydration in Aqueous Solution: Fourier Transform Infrared Studies of HDO Spectra. *J. Chem. Phys.* **2006**, *125*, 204508.

(11) Stoyanov, E. S.; Stoyanova, I. V.; Reed, C. A. The Unique Nature of H+ in Water. *Chem. Sci.* **2011**, *2*, 462–472.

(12) Fournier, J. A.; Wolke, C. T.; Johnson, C. J.; Johnson, M. A.; Heine, N.; Gewinner, S.; Schöllkopf, W.; Esser, T. K.; Fagiani, M. R.; Knorke, H.; et al. Site-Specific Vibrational Spectral Signatures of Water Molecules in the Magic $H_3O^+(H_2O)_{20}$ and $Cs^+(H_2O)_{20}$ Clusters. *Proc. Natl. Acad. Sci.* **2014**, *111*, 18132–18137.

(13) Fagiani, M. R.; Knorke, H.; Esser, T. K.; Heine, N.; Wolke, C. T.; Gewinner, S.; Schöllkopf, W.; Gaigeot, M.-P.; Spezia, R.; Johnson, M. A.; et al. Gas Phase Vibrational Spectroscopy of the Protonated Water Pentamer: The Role of Isomers and Nuclear Quantum Effects. *Phys. Chem. Chem. Phys.* **2016**, *18*, 26743–26754.

(14) Markovitch, O.; Agmon, N. Structure and Energetics of the Hydronium Hydration Shells. *J. Phys. Chem. A* **2007**, *111*, 2253–2256.

(15) Marx, D.; Chandra, A.; Tuckerman, M. E. Aqueous Basic Solutions: Hydroxide Solvation, Structural Diffusion, and Comparison to the Hydrated Proton. *Chem. Rev.* **2010**, *110*, 2174–2216.

(16) Biswas, R.; Tse, Y. L. S.; Tokmakoff, A.; Voth, G. A. Role of Presolvation and

Anharmonicity in Aqueous Phase Hydrated Proton Solvation and Transport. *J. Phys. Chem. B* **2016**, *120*, 1793–1804.

(17) Nibbering, E. T. J.; Elsaesser, T. Ultrafast Vibrational Dynamics of Hydrogen Bonds in the Condensed Phase. *Chem. Rev.* **2004**, *104*, 1887–1914.

(18) Kim, J.; Schmitt, U. W.; Gruetzmacher, J. A.; Voth, G. A.; Scherer, N. E. The Vibrational Spectrum of the Hydrated Proton: Comparison of Experiment, Simulation, and Normal Mode Analysis. *J. Chem. Phys.* **2002**, *116*, 737–746.

(19) Biswas, R.; Carpenter, W.; Fournier, J. A.; Voth, G. A.; Tokmakoff, A. IR Spectral Assignments for the Hydrated Excess Proton in Liquid Water. *J. Chem. Phys.* **2017**, *146*, 5317–224511.

(20) Xu, J.; Zhang, Y.; Voth, G. A. Infrared Spectrum of the Hydrated Proton in Water. *J. Phys. Chem. Lett.* **2011**, *2*, 81–86.

(21) Napoli, J. A.; Marsalek, O.; Markland, T. E. Decoding the Spectroscopic Features and Time Scales of Aqueous Proton Defects. *J. Chem. Phys.* **2018**, *148*, 222833.

(22) Ottosson, N.; Liu, L.; Bakker, H. J. Vibrational Relaxation of the Aqueous Proton in Acetonitrile: Ultrafast Cluster Cooling and Vibrational Predissociation. *J. Phys. Chem. B* **2016**, *120*, 7154–7163.

(23) Dahms, F.; Costard, R.; Pines, E.; Fingerhut, B. P.; Nibbering, E. T. J.; Elsaesser, T. The Hydrated Excess Proton in the Zundel Cation H5O2+: The Role of Ultrafast Solvent Fluctuations. *Angew. Chemie - Int. Ed.* **2016**, *55*, 10600–10605.

(24) Dahms, F.; Fingerhut, B. P.; Nibbering, E. T. J.; Pines, E.; Elsaesser, T. Large-Amplitude

Transfer Motion of Hydrated Excess Protons Mapped by Ultrafast 2D IR Spectroscopy. *Science* **2017**, *357*, 491–495.

(25) Kalish, N. B. M.; Shandalov, E.; Kharlanov, V.; Pines, D.; Pines, E. Apparent Stoichiometry of Water in Proton Hydration and Proton Dehydration Reactions in CH3CN/H2O Solutions. *J. Phys. Chem. A* **2011**, *115*, 4063–4075.

(26) Sigalov, M. V.; Kalish, N.; Carmeli, B.; Pines, D.; Pines, E. Probing Small Protonated Water Clusters in Acetonitrile Solutions By1H NMR. *Zeitschrift fur Phys. Chemie* **2013**, *227*, 983–1007.

(27) Sofronov, O. O.; Bakker, H. J. Energy Relaxation and Structural Dynamics of Protons in Water/DMSO Mixtures. *J. Phys. Chem. B* **2018**, *122*, 10005−10013.

(28) Ramasesha, K.; De Marco, L.; Mandal, A.; Tokmakoff, A. Water Vibrations Have Strongly Mixed Intra- and Intermolecular Character. *Nat. Chem.* **2013**, *5*, 935–940.

(29) Hunger, J.; Liu, L.; Tielrooij, K.-J.; Bonn, M.; Bakker, H. Vibrational and Orientational Dynamics of Water in Aqueous Hydroxide Solutions. *J. Chem. Phys.* **2011**, *135*, 124517.

(30) Van Der Post, S. T.; Hsieh, C. S.; Okuno, M.; Nagata, Y.; Bakker, H. J.; Bonn, M.; Hunger, J. Strong Frequency Dependence of Vibrational Relaxation in Bulk and Surface Water Reveals Sub-Picosecond Structural Heterogeneity. *Nat. Commun.* **2015**, *6*, 8384.

(31) Cringus, D.; Jansen, T. L. C.; Pshenichnikov, M. S.; Wiersma, D. A. Ultrafast Anisotropy Dynamics of Water Molecules Dissolved in Acetonitrile. *J. Chem. Phys.* **2007**, *127*, 084507.

(32) Cringus, D.; Yeremenko, S.; Pshenichnikov, M. S.; Wiersma, D. A. Hydrogen Bonding and Vibrational Energy Relaxation in Water-Acetonitrile Mixtures. *J. Phys. Chem. B* **2004**, *108*,

10376–10387.

(33) Carpenter, W. B.; Fournier, J. A.; Lewis, N. H. C.; Tokmakoff, A. Picosecond Proton Transfer Kinetics in Water Revealed with Ultrafast IR Spectroscopy. *J. Phys. Chem. B* **2018**, *122*, 2792–2802.

(34) Thämer, M.; De Marco, L.; Ramasesha, K.; Mandal, A.; Tokmakoff, A. Ultrafast 2D IR Spectroscopy of the Excess Proton in Liquid Water. *Science* **2015**, *350*, 78–82.

TOC Graphic

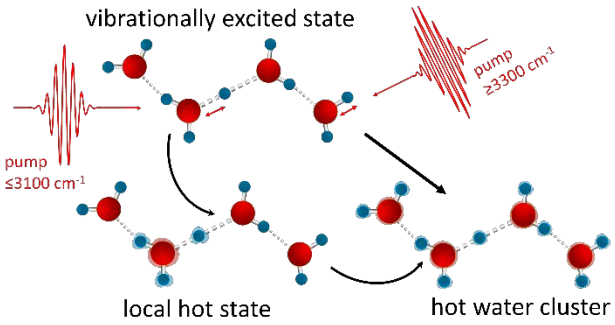
vibrationally excited state
pump
≤3100 cm-1
pump
≥3300 cm-1
local hot state
hot water cluster